Ultrasound in Medicine & Biology 51 (2025) 1250–1260

Contents lists available at ScienceDirect

Ultrasound in Medicine & Biology

journal homepage: www.elsevier.com/locate/ultrasmedbio

Original Contribution

Low Intensity Pulsed Ultrasound Activates Excitatory Synaptic Networks in Cultured Hippocampal Neurons

Fenfang Li [a,*], Hao Jiang [a], Jiawei Lin [a], Chaofeng Qiao [a], George J. Augustine [b,c]

[a] Institute of Biomedical Engineering, Shenzhen Bay Laboratory, Shenzhen, China
[b] Program in Neuroscience & Mental Health, Lee Kong Chian School of Medicine, Nanyang Technological University Singapore, Singapore
[c] Temasek Life Sciences Laboratory, Singapore

ARTICLE INFO

ABSTRACT

Objective: Ultrasound can noninvasively penetrate deep into the brain for neuromodulation, demonstrating good potential for clinical application. However, the underlying mechanisms are unclear. So far most in vitro studies have focused on the activation of individual neurons by ultrasound with calcium imaging. As the focal region of ultrasound is typically millimeter or submillimeter size, it is important to investigate yet so far unclear how the mechanical effects of ultrasound would influence the synaptic circuit activity of neurons.
Methods: Low-intensity pulse ultrasound was used to stimulate cultured hippocampal neurons. Postsynaptic currents were recorded in individual cells with the whole-cell patch-clamp technique. We also simultaneously imaged intracellular calcium, along with neuronal electrical signals, to resolve neuronal network dynamics during ultrasound stimulation.
Results: Excitatory postsynaptic currents (EPSCs) were evoked by ultrasound in high-density neuronal cultures with increased frequency and amplitude, indicating enhanced glutamatergic synaptic transmission. The probability of evoking responses and the total charge of EPSCs increased with ultrasound intensity. Mechanistic analysis reveals that extracellular calcium influx, action potential firing and synaptic transmission are necessary for the responses to ultrasound in high-density culture. In contrast, EPSCs were not enhanced in low-density culture. Simultaneous calcium imaging of neuronal network activity indicates that recurrent excitatory network activity is recruited during ultrasound stimulation in high-density cultures, which lasts over tens to hundreds of seconds.
Conclusion: Our study provides insights into the mechanisms involved in the response of the brain to ultrasound and illuminates the potential to use ultrasound to regulate synaptic function in neurological disorders.

Introduction

The development of noninvasive neuromodulation techniques has provided both the means to investigate intrinsic brain functions, as well as therapeutic strategies to modulate abnormal brain activity in neurological and psychiatric disorders. Two well-established noninvasive approaches are transcranial electric stimulation and transcranial magnetic stimulation. However, these both suffer from limitations in their spatial resolution and penetration depth [1]. In contrast, focused ultrasound (FUS) can noninvasively target deep brain regions with millimeter or better spatial precision without affecting cells along the propagation path [2]. Without genetic or chemical manipulations, and without side effects, transcranial low-intensity FUS has successfully elicited neural activity in different brain regions and behavioral responses in small animals [3–7], large animals [8–10], nonhuman primates [11–14] and human subjects [15–17]. These advantages make FUS promising both for basic neuroscience research and for treatment of brain disorders.

Though there is widespread interest in FUS technology, the mechanisms underlying the ability of FUS to stimulate brain activity are not well understood. FUS may work by activating mechanosensitive ion channels [18–20], transiently creating pores in the plasma membrane [2,20,21], or by actuating intramembrane cavitation that works via a bio-piezoelectric mechanism [22–24]. Ultrasound also affects synaptic transmission [25–27]. In mouse hippocampal slices, low-intensity ultrasound triggers exocytosis mediated by SNARE proteins and thereby enhances synaptic transmission [25]. Low-intensity FUS stimulation of the rat thalamus has been found to increase extracellular concentrations of the neurotransmitters serotonin (5-HT) and dopamine, consistent with FUS stimulating synaptic activity [26]. In a recent study, low intensity ultrasound stimulation was shown to enhance dopamine release in the striatum of a Parkinsons disease mouse model and restore the

* Corresponding author. Institute of Biomedical Engineering, Shenzhen Bay Laboratory, Shenzhen, China.
E-mail address: fenfang.li@szbl.ac.cn (F. Li).

https://doi.org/10.1016/j.ultrasmedbio.2025.04.011
Received 8 February 2025; Revised 21 April 2025; Accepted 22 April 2025

locomotor activity of these mice [27]. However, it is challenging to determine whether such mechanisms are involved in FUS stimulation of brain activity in an in vivo context; this challenge is increased by recent findings of auditory confounds during FUS use in rodents [28–30].

In this study, we used cultured hippocampal neurons to examine the actions of FUS on synaptic transmission and synaptic network activity. We found that a brief bout of FUS triggers a prolonged barrage of excitatory synaptic activity. The magnitude and duration of such responses increased with higher FUS power. Because these excitatory responses could trigger action potentials in the hippocampal neurons, we hypothesized that recurrent excitation of the hippocampal neurons was responsible for the prolonged response to FUS. Consistent with this hypothesis, calcium imaging experiments demonstrated that FUS produced a sequential activation of many neurons, with a time course comparable to that of the prolonged barrage of excitatory synaptic transmission produced by FUS. Our results indicate that ultrasound can produce sustained, recurrent excitation of neural networks and such actions may underlie the ability of FUS to stimulate the brain in vivo. These results help to bridge our understanding of how FUS excitation of individual neurons can lead to neuronal network activation in the in vivo context.

Results

Acoustic streaming induced by ultrasound

The goal of our experiments was to characterize the effects of ultrasound on cultured mouse hippocampal neurons. For this purpose, we integrated a 25 MHz point-target-focus ultrasound transducer into an inverted microscope equipped with electrophysiology capabilities (Fig. 1a). During the experiment, the ultrasound transducer was operated in pulse mode with a duty cycle of 5%, a pulse repetition frequency of 5 Hz, and a total duration of 20 s (Fig. 1b). A needle hydrophone was used to measure the acoustic fields generated by such low-intensity, pulsed ultrasound (LIPUS; Fig. S1). These inputs corresponded to pressures ranging from 0.59 to 0.91 MPa and their corresponding spatial peak-time average intensities, I_{SPTA}, ranged from 0.58 to 1.41 W/cm^2 (Fig. 1c). To determine fluid shear stress exerted on cells, acoustic streaming was empirically measured by PIV (Fig. 1d). Time-lapse images of acoustic streaming, taken from the bottom view, showed significant fluid flow around the focal region of the ultrasound transducer. The flow velocity as well as the spatial range of flow increased with ultrasound intensity, as also shown by Fig. S2. Even though the duration of individual LIPUS pulses was 10 ms and the time interval between the pulses was 200 ms, the maximum streaming velocity occurred after the ultrasound pulses had ceased, at 10.9 ms for I_{SPTA} of 0.58 W/cm^2 and 12.5 ms for I_{SPTA} of 1.21 W/cm^2, and the streaming flow lasted for more than 26.5 ms for I_{SPTA} of 0.58 W/cm^2 and 200 ms for I_{SPTA} of 1.21 W/cm^2. This result indicates that the mechanical effects associated with acoustic streaming lasted much longer than the individual LIPUS pulses. Further PIV measurements of the time evolution of fluid velocities at different locations and the comparison between different ultrasound intensities are shown in Figure S2. Numerical modeling with COMSOL Multiphysics software revealed the predicted flow field of acoustic streaming and the distribution of acoustic pressure from a side view (Fig. 1e and Fig. S3). It shows that the emitted ultrasound beam focused on the cover slip of the recording chamber, where cells were located, and was reflected there. The velocity of acoustic streaming was calculated to be maximal at the focal point and increased with ultrasound intensities. More details about our numerical modeling results, including the acoustic pressure, acoustic body force and acoustic streaming at different ultrasound intensities, are shown in Figure S3.

LIPUS evokes synaptic activity in cultured neurons

We next used patch clamp recordings of ionic currents to characterize the effects of LIPUS on cultured hippocampal neurons. These recordings were made in voltage-clamp mode, with the cellular membrane potential held at −70 mV. We found that healthy neuron status was essential to successful patching. In 20 out of 28 successful patching experiments, LIPUS application generated a barrage of apparent postsynaptic currents in neurons. Figure 2a shows an example of the high-frequency events that were evoked by LIPUS stimulation (0.46 W/cm^2).

We first identified the nature of the postsynaptic currents before quantifying it. Several lines of evidence indicate that these events are excitatory postsynaptic currents (EPSCs) produced by the release of the neurotransmitter glutamate. Frist, they were abolished when LIPUS was applied in the presence of a glutamate receptor antagonist, kynurenic acid (Fig. 2b). This indicates that they are EPSCs produced by activation of ionotropic glutamate receptors. Second, they were not observed in an extracellular solution containing no calcium ions (Fig. 2c). It is known that release of glutamate and other neurotransmitters requires influx of extracellular calcium [31,32], identifying them as EPSCs resulting from glutamate release from presynaptic terminals. Third, they were abolished by treatment with tetrodotoxin (TTX, 1 μM; Fig. 2d), a well-known blocker of the voltage-dependent sodium channels that underlie neurotransmitter release evoked by presynaptic action potentials (APs). Finally, their rapid decay kinetics (< 10 ms time constant) is typical of glutamatergic EPSCs [33] (Fig. 2e). We therefore conclude that these events were a barrage of EPSCs caused by release of glutamate that was evoked by APs in presynaptic neurons that innervated the neurons that we were recording from. More evidence is shown in Figure S4 at different ultrasound intensities to support our identification.

It is worth noting that APs are >10 times faster than EPSCs. They are also much larger in amplitude than individual EPSCs. Thus, it is easy to distinguish APs from EPSCs. In some cases, the EPSCs evoked by LIPUS were large enough to evoke APs in the postsynaptic neuron, which were readily identifiable by their larger amplitudes and briefer time courses (see Fig. 2f) compared to the EPSCs (Fig. 2e). An example of such a response is shown in Figure 2g. In this experiment, the response to LIPUS (0.87 W/cm^2) initially consisted of a barrage of EPSCs which, in turn, generated a series of APs. Although a voltage-clamped neuron should, in principle, be prevented from firing APs, it is well-known that large depolarizations can evoke APs in distal neuronal processes whose membrane potentials are not well-controlled by the somatic voltage clamp [34,35]. These APs were blocked by treatment with TTX (Fig. 2h). The frequency of these postsynaptic APs was reduced both by application of kynurenic acid (Fig 2i) or calcium-free conditions (Fig 2j), consistent with them arising from EPSCs. However, occasionally low-frequency AP firing could still be evoked at the onset of stronger LIPUS stimuli; we attribute these events to direct excitation of the patched neuron by LIPUS.

One striking characteristic of these responses to LIPUS was their persistence. The frequency of EPSCs gradually increased during the LIPUS stimulation and progressively decayed afterwards, with EPSCs observed for approximately a minute after the LIPUS was switched off (Figs. 3a1 and 3a2). The same was true for LIPUS-induced APs: these, too, outlasted the stimulus and as observed for the barrage of underlying EPSCs (Figs. 3b1 and 3b2), was sustained for approximately a minute after stimulation ceased (Fig. 3b3). Thus, the mechanism responsible for the barrage of EPSCs persists for almost a minute after LIPUS.

We next examined the effects of different ultrasound intensities on the response of the cultured neurons to LIPUS. Figures 4a–c show three representative examples of current measurements made during LIPUS stimulation with increasing I_{SPTA}, where individual cells were voltage-clamped at a holding potential of −70 mV. In these experiments, ultrasound intensity was gradually increased until sustained EPSC or AP responses were evoked, with at least a 100 s interval between stimuli. Although APs are generally all-or-none in amplitude, we often observed a time-dependent reduction in AP amplitude during the prolonged responses to LIPUS (Figs. 4a–c). This was due to the well-known phenomenon of AP amplitude adaptation [36], with possible additional

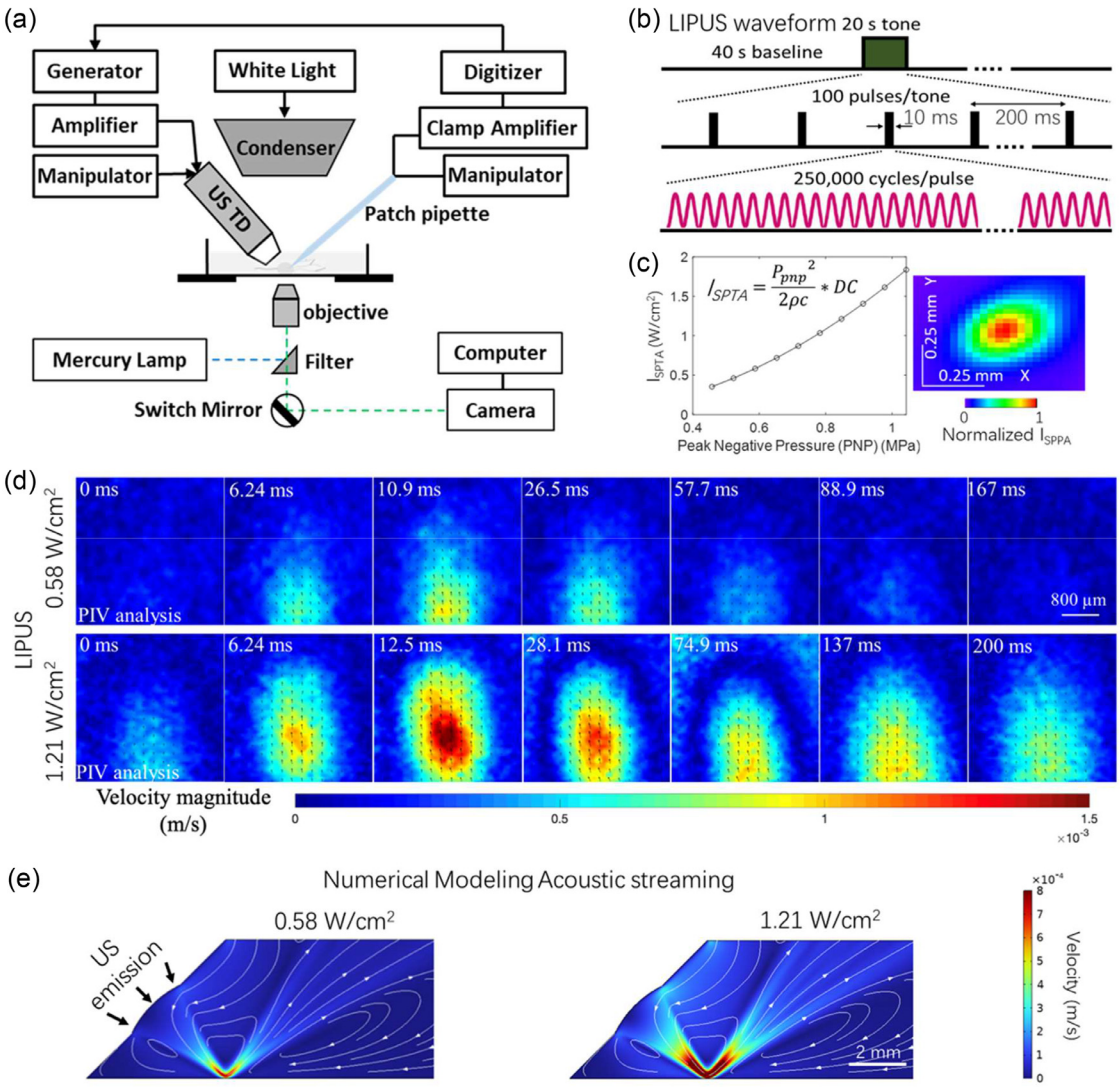

Figure 1. Experimental System. (a) Schematic illustration of the experimental platform for ultrasound stimulation, voltage clamp and calcium imaging of cultured neurons. A modulated sinusoidal signal was generated by a function generator, which was amplified by a 50-dB power amplifier to drive the ultrasound transducer. The position of the ultrasound transducer and the patch pipette were manipulated by three-axis micromanipulators. The timing of ultrasound stimulation and voltage clamp recordings were controlled by a digitizer. Camera was used for calcium imaging. (b) LIPUS waveform used in the experiment. 25 MHz fundamental frequency (40 ns period), pulse repetition frequency 5Hz, duty cycle (DC) 5%, total burst duration 20 s. (c) Peak negative pressure (P_{pnp}) used in this study and the corresponding spatial peak time average intensities, I_{SPTA}. Intensities were calculated using the equation shown in the inset, where ρ is the density of external solution, c is speed of sound in external solution, DC is duty cycle. The measured acoustic focus in the X–Y plan is shown on the right with I_{SPPA} denoting the spatial peak pulse average intensities. (d) Time-lapsed visualization and analysis of the acoustic streaming, from bottom view, by PIV experiments done at two different ultrasound intensities (I_{SPTA} of 0.58 and 1.21 W/cm^2). (e) Numerical simulation of acoustic streaming produced by ultrasound with COMSOL multiphysics.

contributions from time-dependent changes in spatial control of membrane potential [34,35].

The threshold level of LIPUS required to evoke such responses varied from experiment to experiment and ranged from 0.35 to 1.41 W/cm^2. In general, the probability of evoking EPSC and APs increased as ultrasound intensity was increased: in all the examples shown in Figure 4, lower LIPUS intensities evoked smaller and briefer responses – consisting of fewer EPSCs and APs - than were observed when the stimulus intensity was increased. It is worth noting that once sustained EPSC or AP responses were evoked, equally robust responses could not be evoked again with the same or higher US intensities applied within several hundred seconds (see SI Fig. S5). Therefore, we avoided analyzing such refractory responses. Considering the results of all experiments (N = 28), the probability of LIPUS enhancing EPSC activity increased with ultrasound intensity, beyond an apparent threshold of around 0.35 W/cm^2 (40% of cells were responsive at this intensity), and was maximal at approximately 1 W/cm^2 (Fig. 4d). To characterize the magnitude of responses at different LIPUS intensities, we measured the total amount of charge (temporal integral of current, also can be defined as area under the curve for the current trace) associated with the barrage of LIPUS-evoked synaptic activity. The total amount of charge evoked by medium (0.72–1.03 W/cm^2) or higher intensity (1.21–1.61 W/cm^2) LIPUS was significantly larger than that measured without US stimulation, while responses measured during lower levels of LIPUS (0.35–0.58 W/cm^2) were smaller. This was true whether charge measurements included only EPSCs (Fig. 4e) or charge associated with both EPSCs and APs (Fig. 4f). We conclude that the magnitude of the synaptic response to LIPUS depends upon the intensity of the US stimulus. This relationship was abolished in cells treated with TTX, kynurenic acid, or calcium-free saline solution (Fig. 4g and Fig. S4), again indicating the central role of glutamate release at excitatory synapses in these responses.

Because synaptic transmission is sensitive to heat [37,38], we employed two different methods to ask whether our LIPUS protocol affected the temperature of the neurons and their surrounding medium.

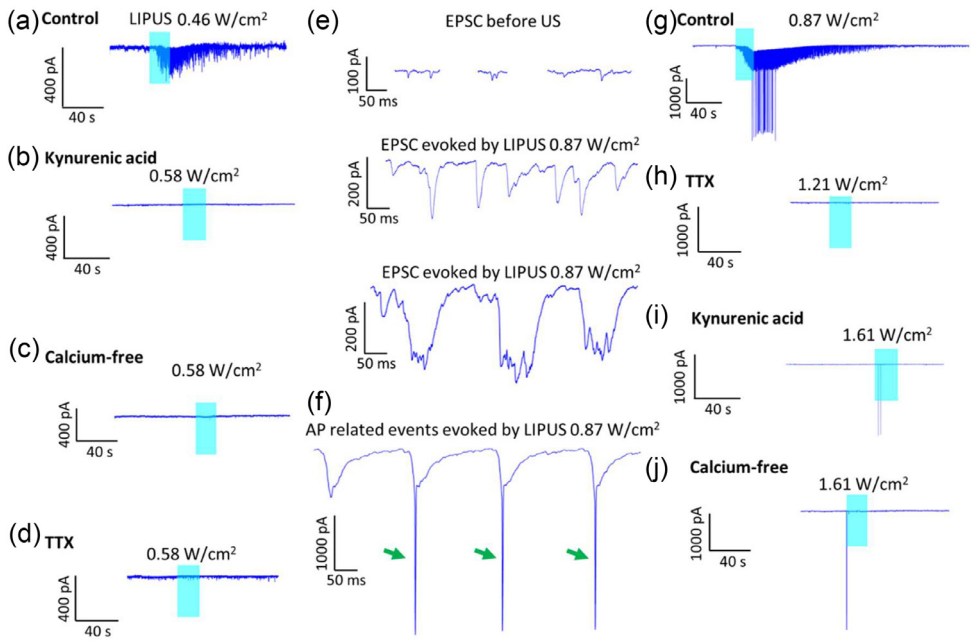

Figure 2. LIPUS evoked excitatory postsynaptic currents (EPSCs) in high-density neuronal cultures. Example current traces from a voltage-clamped neuron stimulated by LIPUS in normal external medium, medium with kynurenic acid (a glutamate receptor antagonist), calcium-free medium and medium with TTX at lower (a–d) and higher (g-j) ultrasound intensities. (e) Typical examples of EPSCs before ultrasound application, as well as evoked by ultrasound when there were no APs. (f) Examples of APs-related current events (arrows) evoked by ultrasound.

First, temperature was measured with a thermocouple and the temperature change associated with LIPUS was negligible, within 0.1–0.2 degrees (Fig. S6). Second, because temperature measurements with a digital thermometer could underestimate ultrasound-induced heating, we also employed an infrared camera to more accurately assess temperature changes at the target following 20 s of LIPUS. The results again showed negligible heating effects of a fraction of a degree or less (Fig. S7). Such negligible heating effects are likely due to the low (5%) duty cycle used in our study. Thus, the prolonged neuronal activation that we observed in response to LIPUS, persisting for tens of seconds poststimulation, was unlikely to be caused by neuronal heating. To ask whether neurons were being damaged by LIPUS, we measured the membrane holding current, which is a very sensitive measure of neuronal leakiness. We found that LIPUS intensities as high as 1.61 W/cm^2 had little effect on membrane holding current (Fig. S8), indicating that the prolonged response to LIPUS was not due to neuronal damage.

LIPUS response depends on neuron density

A hypothesis about the cause of the protracted responses to LIPUS comes from a detailed examination of these responses. As described above, in high-density cultures LIPUS evoked robust barrages of EPSCs

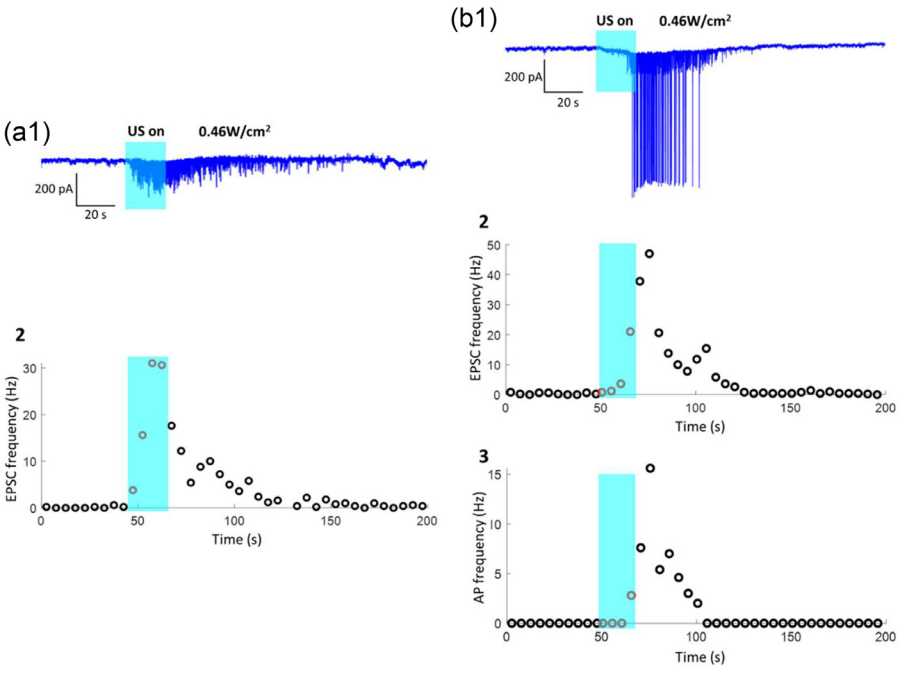

Figure 3. Ultrasound (blue shading) evoked sustained excitatory postsynaptic currents (EPSCs) and action potentials (APs) in high-density hippocampal neuron cultures. (a1–b1) Examples of current responses to ultrasound stimulation (0.46 W/cm^2) in two independent experiments (both cells held at −70 mV). (a2) Time course of changes in EPSC frequency measured in the experiment shown in a1. (b2–b3) Time course of LIPUS-induced changes in EPSCs frequency (b2) and AP frequency (b3), measured in the experiment shown in b1.

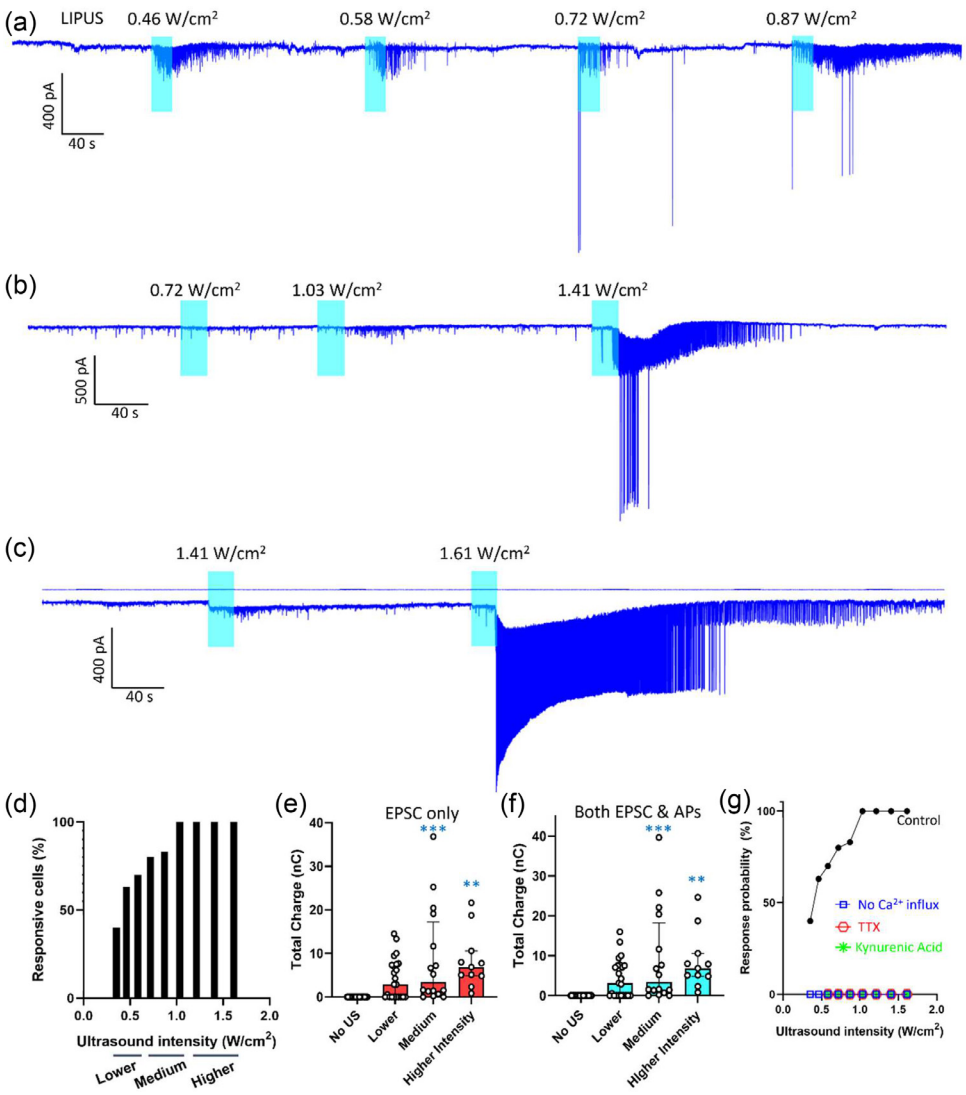

Figure 4. (a–c) Three different examples of current responses to LIPUS stimulation measured in high-density neuron cultures. In each case, ultrasound intensity was gradually increased until maximal sustained increases in EPSCs and/or APs occurred. Cells were held at a potential of −70 mV. (d) Effect of LIPUS intensity on the probability of evoking EPSC activity in individual neurons. N = 5, 8, 10, 5, 6, 5, 5, 3, 3 for LIPUS with intensity ranging from 0.35 to 1.61 W/cm^2, respectively. (e–f) To quantify LIPUS responses, the total charge of EPSCs alone (e) and charge of both EPSC and APs (f) was determined at different ultrasound intensities. No US group, N = 24. Lower intensity LIPUS: 0.35–0.58 W/cm^2, N = 23. Medium intensity LIPUS: 0.72–1.03 W/cm^2, N = 16. Higher intensity LIPUS:1.21–1.61 W/cm^2, N = 11. The bar graph indicates the median value with the error bars denoting interquartile range; three consecutive LIPUS intensities were binned for better visualization. One-way ANOVA multiple comparisons were used for statistical comparisons; both (e) and (f) exhibited statistically significant ($p < 0.001$) effects of LIPUS intensity. The asterisks depicted the statistical significance between specific ultrasound group and control group with no ultrasound. ** $p < 0.01$, *** $p < 0.001$. (g) Relationship between probability of observing LIPUS responses (enhanced EPSC frequency) and LIPUS intensity in individual neurons in normal control medium (the same control group as in Fig. 4D), calcium-free medium, medium with TTX added to block APs, and medium containing kynurenic acid to block excitatory synaptic transmission. N = 2,2,9,9,9,9,7,6,5 for calcium-free medium, N = 4,4,4,4,4,3,3 for medium with TTX, and N = 7,5,6,6,6,5,6 for Kynurenic Acid treated cases for the corresponding US intensities as shown in panel G.

and APs. Figure 5a shows another example of the response to LIPUS under these conditions: sustained EPSC activity and AP firing were observed during and following US stimulation. The inset on the right of Figure 5a is an expanded view of part of the response during the time that AP firing was initiated. This view reveals repetitive bursts of compound EPSCs, each of which lasts for approximately 0.2 s and attains a peak value of approximately 500 pA. EPSCs bursts are multiple EPSC events with shorter intervals than the control condition; because of the duration of individual EPSCs, the short inter-event interval caused EPSCs to ride on top of each other to yield bursts of compound EPSCs [39]. As the bursts increased in amplitude, APs were also generated. Such bursts are often observed in high-density cultures of neurons and are thought to arise from the recurrent activity of excitatory synaptic networks formed between the neurons [40,41]. Thus, it is possible that LIPUS produces sustained EPSC and AP activity by activating such recurrent excitatory circuits.

One line of evidence supporting this possibility came from measurements made in cultures which had a lower density of neurons (~20,000 cells/coverslip, compared to ~80,000/coverslip for high-density cultures). In such low-density cultures, responses to LIPUS were greatly attenuated. Figure 5b shows measurements from two neurons from different low-density cultures during LIPUS application. Even at higher ultrasound intensities (1.03 and 1.21 W/cm^2) no bursts of EPSCs were observed. Aside from a few low-frequency EPSCs, there were a small number of APs observed, which presumably reflected LIPUS directly stimulating AP firing in these neurons. Similar results were observed in a total of 7 experiments. To further evaluate the role of neuronal density in the response to LIPUS, we also examined the effects of

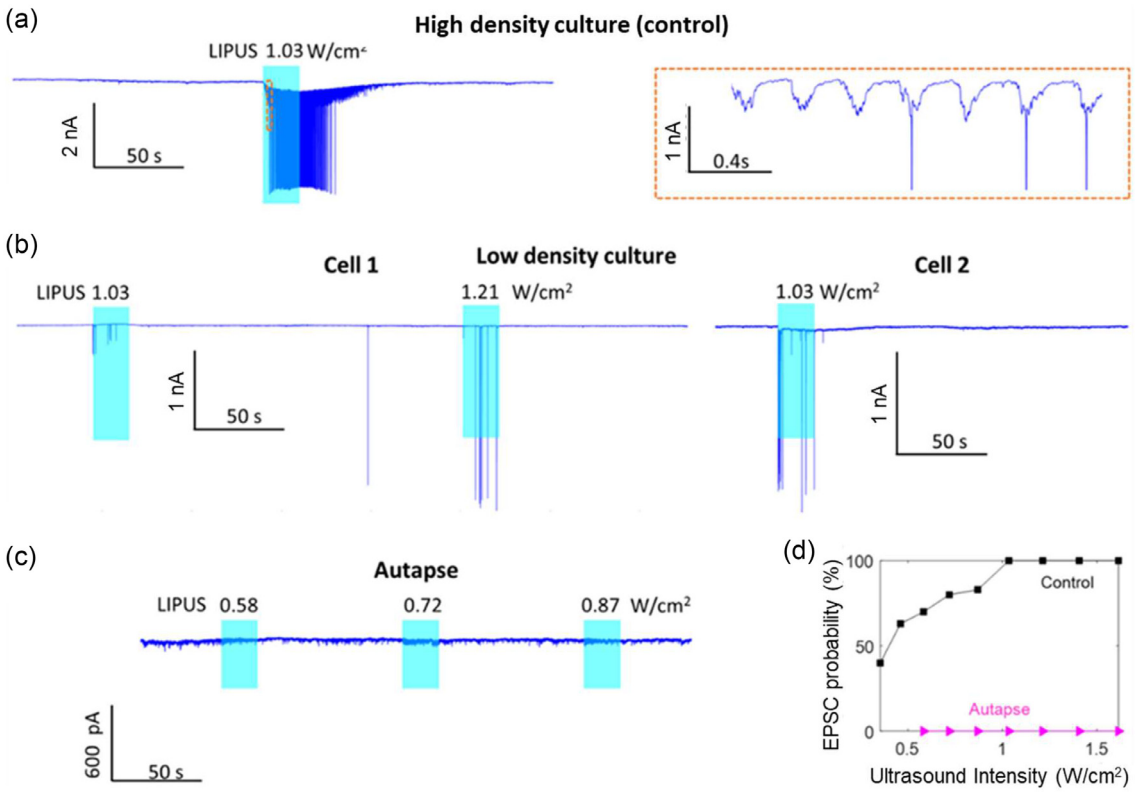

Figure 5. The influence of neuronal density on the ability of LIPUS to evoke EPSCs. (a) Example current response of a neuron to LIPUS in high-density culture conditions. Inset on the right shows an expanded view of part of this response. (b) Current responses to LIPUS recorded in two individual neurons in low-density culture conditions. (c) Lack of current responses to LIPUS stimulation in a microisland-cultured autaptic neuron. (d) Probability of LIPUS enhancing ESPC frequency at increasing I_{SPPA} in autaptic neurons, compared to neurons in high-density cultures (the same control group as in Fig. 4d). N = 4–7 for autaptic neurons and 4–10 for the high-density control group.

LIPUS in single-neuron microisland cultures, where the solitary neuron forms "autapses" with itself [42]. In 37 recordings from neurons in such conditions, no EPSC or AP activity was evoked by LIPUS (Fig. 5c). Across the entire range of LIPUS intensities, the probability of US evoking ESPCs in autaptic neurons was zero, compared to 40%–100% in high-density cultures (Fig. 5d).

Taken together, our results indicate that neuronal density has an important influence on the response of cultured neurons to LIPUS. This indicates that the degree of network connectivity is a key determinant for this response and is consistent with the hypothesis that the response arises from recurrent synaptic excitation within the networks formed by the cultured neurons.

Recurrent synaptic circuit activity underlies the response to LIPUS

The recurrent network hypothesis predicts that LIPUS should cause sustained activation of numerous neurons within the high-density cultures. We tested this prediction by using calcium imaging to monitor the activity of many neurons simultaneously. Electrical excitation of neurons is associated with transient elevation of intracellular calcium concentration, allowing fluorescent indicators to visualize calcium signals that serve as a surrogate of AP firing [43,44]. In these experiments, we loaded neurons with the calcium indicator dye, fluo-4, and imaged many cells simultaneously by using a 10 × low-magnification lens with a wide field of view. A typical example of the calcium signals produced in neurons in a high-density culture in response to LIPUS is shown in Figure 6; the panels in Figure 6a show calcium signals evoked by LIPUS from fluorescence images taken at the indicated times, while Figure 6b shows pseudo-colored surface plots that make it easier to discern the location of active neurons. Only neurons with discernable calcium signals are shown, for better visualization of the spatial propagation of calcium response. When the US was switched on at t = 0, only a few cells on the top left of the field exhibited calcium responses; these cells were located within the ultrasound focus. This activity then gradually spread from these cells to neurons throughout the image field by the end of the LIPUS stimulation (t = 19.8 s). Similar widespread neuronal activation in response to

LIPUS was seen in a total of 26 experiments. We observed that calcium responses were initiated at random locations in different experiments. This is consistent with the size of the ultrasound focus (around 0.4 mm in diameter; Fig. 1), which caused all the cells in the image field to be within the focal region.

Intracellular calcium levels remained high for a minute or two after the stimulus ended; this indicates sustained activation of the neuronal network, as predicted by the hypothesis. To define the temporal relationship between neuronal activity and the EPSC barrage triggered by LIPUS, we performed simultaneous voltage clamp measurements and calcium imaging in high-density neuron cultures. Figure 7a shows the current response of a patched neuron, while the inset shows a fluorescence image of fluo-4 loaded neurons within the image field; the location of the patch pipette is diagrammed in white, and the patched neuron is indicated by a blue circle. The location of some of the neurons that exhibited calcium responses to LIPUS are labeled in red circles and the time course of their calcium responses are shown in Figure 7b. Cells #1 to #9 are numbered in order of their latency to produce calcium responses to LIPUS, while the calcium response of the patched cell is indicated by the blue trace in Figure 7b. Because they are shown on the same time scale, it is possible to compare the timing of the current responses of the patched cell (Fig. 7a) with the calcium responses of cells #1 to #9 (Fig. 7b). The calcium response of cell #1 coincided with both the start of LIPUS stimulation and the barrage of EPSC activity. As more cells became active during LIPUS stimulation (Fig. 7b), the number of

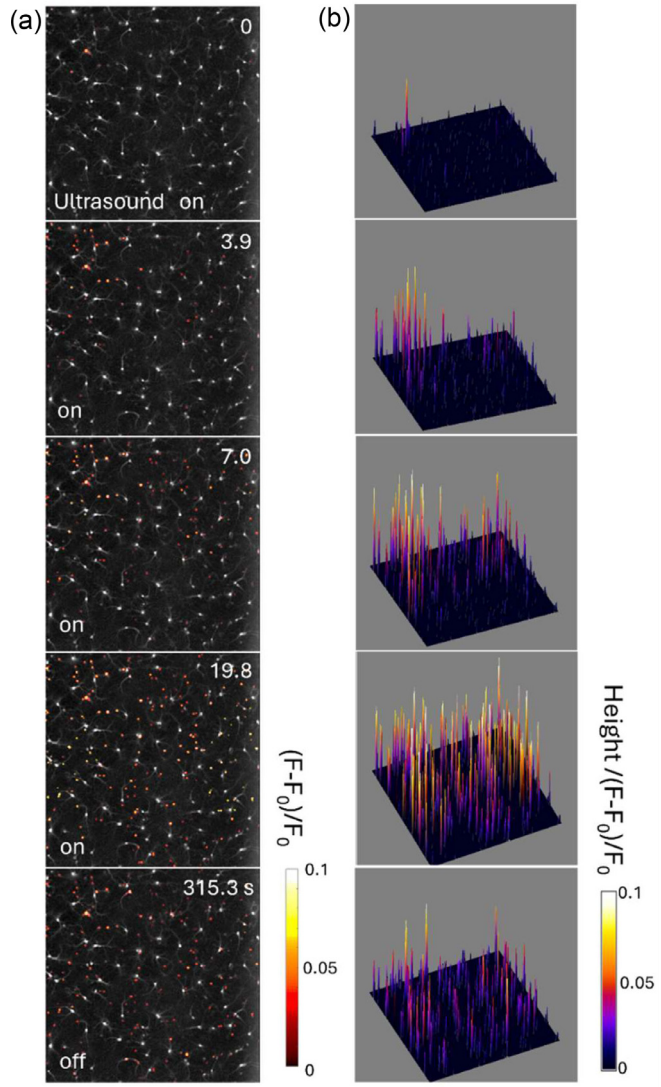

Figure 6. Calcium imaging of neuronal activity in a high-density culture in response to LIPUS with I_{SPTA} of 1.21 W/cm^2. (a) Time-lapse images revealing the spatiotemporal changes in calcium signals at the indicated times after initiating LIPUS stimulation; LIPUS was applied from 0 to 20 s. Gray-scale image illustrates the resting fluo-4 fluorescence of all cells within the image field, while pseudocolors (scale at lower right) depict rises in calcium associated with LIPUS. (b) 3D surface plot of the calcium responses shown in (a). The height and pseudocolor (scale at lower right) indicate the magnitude of changes in calcium induced by LIPUS.

EPSCs increased and a few APs appeared in the patched cell (Figs. 7a, c). These APs were presumably responsible for the calcium signals observed in the patched cell (blue trace in Fig. 7b). After LIPUS was switched off, the calcium signals of the network gradually subsided; this correlated with the gradual reduction in number of EPSC events in the patched cell (Fig. 7d). The cell-averaged calcium signal of the network elevated during LIPUS stimulation, reached its peak a few seconds after LIPUS and gradually decayed afterwards (Fig. 7e). The time course of the averaged Ca^{2+} response roughly parallels that of the EPSC barrage (Fig. 7d), though it recovered somewhat more slowly than the EPSCs (see Discussion). Similar results were observed in a total of 7 experiments that showed elevated EPSC activity in the patched neurons in response to LIPUS stimulation. In 2 other experiments, we observed widespread neuronal activation that was not associated with enhanced EPSC activity in the patched cell. In these cases, it appears that the patched cell was not part of the network of activated neurons. Although the cumulative effect of LIPUS in time may contribute to the intracellular Ca^{2+} response of cells, the sequential propagation of Ca^{2+} signaling and the sustained EPSC activity in the patched neuron in Figures 6 and 7 indicate that neural network transmission is involved.

In summary, our calcium imaging results indicate that (1) there is recurrent activation of a network of neurons in response to LIPUS; and (2) such neuronal activity is temporally coincident with the barrage of EPSCs recorded in the patched cell in response to LIPUS. Both findings are predicted by the hypothesis. When taken together with our observation that the barrage of EPSCs arises from APs in presynaptic neurons (Figs. 2 and 4), our results lead us to conclude that LIPUS causes the EPSC barrage via recurrent activation of an excitatory neural network within the culture.

Discussion

Neurons in the brain are interconnected by synapses to form intricate networks, which allow the brain to perform specific functions and respond to changes in the external environment. We have found that FUS application increases the activity of excitatory synapses, which in turn leads to recurrent synaptic network activity that greatly outlasts the duration of US stimulation. Our results yield new insights into the actions of the US on brain tissue and suggest a possible mechanism for the ability of US to modulate brain activity in vivo.

Most studies investigating the cellular mechanisms underlying US neuromodulation have employed calcium imaging [45–49], which provides good spatial resolution but provides little information about how (or whether) such calcium signaling affects neuronal function. Our electrophysiological analysis, based on whole-cell patch-clamp recording before, during and after 25 MHz ultrasound application, yielded high temporal resolution and precise information about the generation of APs, as well as subthreshold events, such as EPSCs, that could not be detected by calcium imaging. While several recent studies have obtained electrophysiological recordings during application of high US frequencies (30 and 43 MHz), these measurements were limited to analysis of AP dynamics in single cells and did not consider postsynaptic currents or integration of signals across neuronal networks [50–52]. Many other previous studies have focused on responses of cells expressing exogenous ion channels that are sensitive to ultrasound [50,52,53]. Considering the effects of FUS on native neurons and neuronal networks expressing only endogenous ion channels – as we have done - provides important insights that are directly relevant to FUS neuromodulation in vivo and offers potential insights into the use of FUS for clinical applications. Although our study used ultrasound stimulation at 25 MHz—a frequency much higher than used for human transcranial stimulation (<1 MHz)—calcium imaging experiments demonstrate that Ca^{2+} responses can be evoked in neuronal cultures at frequencies much lower than 25 MHz: 2.25 MHz (Fig. S9) and 0.3 MHz [18]. This suggests that the mechanistic insights gained from our observations of responses to 25 MHz ultrasound may also extend to ultrasound stimulation *in vivo*, perhaps even in humans.

A recent study reported artifactual effects of FUS stimulation related to FUS-induced electrode resonance or displacement; such effects could introduce depolarizing leak currents, particularly at sub-MHz frequencies [54]. However, at the higher FUS frequency that we examined (25 MHz), no such displacement of the recording electrode was observed. This is consistent with other reports of successful electrophysiological recordings at high (30 and 43 MHz) FUS frequencies [50–52]. It is worth noting that when we tried 2.25 MHz fundamental frequency ultrasound, we could only get stable recordings at very low acoustic pressure and the recordings were prone to disruption by mechanical vibrations. Therefore, we employed 25 MHz fundamental frequency in our experiments.

Displacement of the recording electrode by FUS may also apply mechanical stimulation to an individual neuron, which could then initiate network activity. However, this was not the case: our results show that the patched cell did not get leaky (Fig. S8) and was never the first

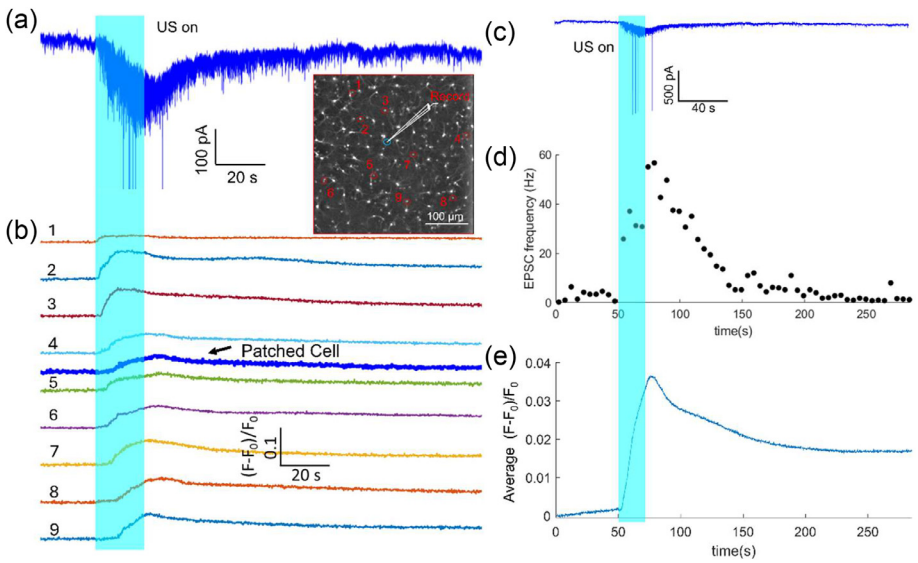

Figure 7. Simultaneous calcium imaging and voltage-clamp recording to compare the timing of EPSC and network responses to LIPUS with I_{SPTA} of 1.21 W/cm^2 (applied at shaded bars). (a) Current response of an individual neuron within a high-density culture. Inset: Fluorescence image indicating location of the patch pipette (in white), with the patched cell within the blue circle. Red circles depict the location of cells exhibiting rise in calcium in response to LIPUS; cells #1 to #9 are numbered in the order which their calcium responses started. (b) Time course of calcium responses of the individual cells identified in the inset of (a), temporally aligned with the current trace shown in (a). (c–e) Comparison of time course of EPSC and calcium responses. (c) Low-gain display of the current response shown in (a), to allow visualization of APs. (d) Time course of the changes in EPSC frequency measured in the patched cell. (e) Time course of calcium response averaged over many cells in the image field.

cell to generate calcium signals (Fig. 7b). Instead, we found that patched cells exhibited increased EPSC activity that must have arisen from LIPUS activation of other presynaptic cells. Further, in some experiments we did not use recording electrodes but still observed network calcium responses to LIPUS that were comparable to those measured in experiments that employed both calcium imaging and electrodes. Another concern is the potential for the recording electrode to introduce cavitation nuclei; this is unlikely in our case, because we used 25 MHz fundamental FUS frequency and the cavitation threshold is hard to reach at this high frequency with low intensity FUS [55]. In summary, we are confident that neither electrode movement nor cavitation caused the responses that we observed.

It is worth noting that the inhibition of neuronal activity by LIPUS has also been reported, e.g., for suppression of epilepsy [56,57]. These studies usually employ ultrasound with fundamental frequency < 1MHz and PRF of 100–1.5 KHz, which is much larger than the PRF used in our study (5 Hz). Because activation of interneurons will inhibit synaptic networks, it is also possible that different ultrasound stimuli could preferentially activate interneurons. Finally, stimulating neurons for too long or too frequently can make them inactive, due to depolarization block [58]. Thus, whether LIPUS evokes excitatory or inhibitory effects on neuronal networks may well depend upon the ultrasound stimulus employed and this must be kept in mind in future studies.

A striking observation in our experiments was the prolonged responses of synaptic circuits to brief application of LIPUS. This prolonged response is consistent with our numerical simulations of acoustic streaming and our experimental measurements of streaming via particle image velocimetry, which indicate that the mechanical effects associated with acoustic streaming last much longer than the individual LIPUS pulses (Fig. 1). In addition, acoustic streaming velocity also rose with higher ultrasound intensities (Fig. S2), as did the neuronal responses to ultrasound (Fig. 4). These correlations suggest that acoustic streaming may at least partially underlie the synaptic effects of LIPUS.

One of the most important lines of evidence supporting our recurrent network model for the response to FUS is the observation that both the synaptic responses of individual neurons and the recurrent network activity of other neurons in the culture greatly outlast the duration of the LIPUS stimulus (Fig. 7). However, there was a quantitative mismatch between these responses: the network calcium signals (Fig. 7e) somewhat outlasted the EPSC barrage (Fig. 7d). There are several possible reasons for this mismatch. First, we would expect the EPSCs to decline more rapidly because of the nonlinear (4th power) relationship between Ca^{2+} and transmitter release probability [59]. Second, it is likely that synaptic depression occurs over the prolonged time course of the response, which will deplete the synaptic vesicles and lower glutamate release even though Ca^{2+} concentration remains elevated [60]. Finally, it is possible that the cells with the most protracted Ca^{2+} signals may not be the ones that are driving the network reverberations. For these reasons, the data shown in Figure 7 represent strong support for the recurrent network model of LIPUS stimulation. It is worth noting that a recent study reported 15 min of 1-MHz LIPUS stimulation could facilitate neuronal activity for about 30 min in cultured hippocampal neurons, where increased frequency of both spontaneous APs and spontaneous excitatory synaptic currents (sEPSCs) were observed by patching the neurons within 5min after LIPUS application [61]. Both their whole-cell recordings after 1 MHz LIPUS and our measurements before, during and after 25 MHz ultrasound stimulation indicated that LIPUS stimulation evokes sustained neuronal activity that persists after stimulation has stopped. It is reasonable to expect that longer stimulation would yield a more prolonged response in their study.

A previous study of cultured cortical neurons indicated that LIPUS activates specific calcium-selective mechanosensitive ion channels, resulting in a gradual build-up of calcium that is amplified by calcium- and voltage-gated channels to generate a burst-firing response [18]. Such responses are consistent with, and could even be responsible for, the recurrent excitatory neural network that we observed. Further, the recurrent network activity that we observed could be responsible for the induction of long-lasting synaptic plasticity, such as long-term potentiation or depression, by transcranial focused ultrasound [36,62]. These long-term synaptic changes are connected to learning and memory processes that play important roles in brain function. Thus, our results provide mechanistic insights into the actions of transcranial focused ultrasound in vivo.

In conclusion, our results establish that LIPUS can activate neuronal network activity, EPSCs and glutamatergic synaptic transmission in high-density cultures of neurons. Such activation lasts for tens to hundreds of seconds and is enhanced by higher levels of LIPUS. Extracellular calcium influx, APs firing, synaptic transmission, neuron network connectivity and the recurrent excitatory network activity are all necessary for LIPUS-activated EPSCs. Our results provide insights into the mechanism of LIPUS-induced neuromodulation and reveal strategies for utilizing LIPUS to regulate synaptic transmission and neurotransmitter release in vivo, with the potential for intervention in neurological disorders such as Parkinson's disease and Alzheimer's disease.

Materials and methods

Hippocampal neuron cultures

Newborn pups (postnatal day 0–1) from wild-type mice were used to prepare hippocampal neurons. The procedures used to maintain and use

these mice were approved by the Institutional Animal Care and Use Committee of Nanyang Technological University. High-density and low-density cultures of hippocampal neurons were prepared as described in Ref. [63] and used 10–18 days later to allow the neurons to mature. The seeding concentration into 24 wells plates was around 80,000 cells/mL for high-density cultures and 20,000 cells/mL for low-density cultures. Neurons were seeded on 12-mm-diameter #1 round cover slips precoated with poly-D-lysine to enhance cell adhesion, placed in a 24-well plate. For experiments, each cover slip was carefully transferred to a custom glass-bottom recording chamber (Fig. S6A). The chamber provided a larger, more accessible workspace than a single well of the 24-well plate, facilitating simultaneous ultrasound stimulation and electrophysiological recordings. Microisland cultures of autaptic neurons were prepared with the addition of glia feeder cells to support neuronal survival [42]. After 14-18 days, these autaptic neurons were used for electrophysiological recording

Ultrasound setup and parameter settings

Ultrasound waveforms were designed by a function generator (Rigol DG972) and gated by the TTL pulse from a digitizer (Digidata 1440A) via pClamp software. The waveforms were amplified by a 75-W RF power amplifier (E&I, model A075). A 25 MHz transducer (V324-N-SU-F0.5IN, Olympus) was used to stimulate neuron cultures. The transducer output was characterized by a needle hydrophone (ONDA HNA-0400) measurements in 0.05-mm increments in y and z directions, and 0.25 mm increments in x direction in a large tank filled with water. After finding the focal point, the output pressure was measured there at different input voltages (Fig. S1).

We used 25 MHz high-frequency ultrasound to eliminate vibrations of the recording electrodes, ensuring stable patch-clamp recordings. To minimize thermal effects, we employed a low duty cycle of 5%. Our choice of parameters was informed by prior work from Liao et al. (2021) [64], who demonstrated that pulse lengths of 10–100 ms effectively activate the mechanosensitive ion channel Piezo1 via acoustic streaming-induced shear stress, using a total ultrasound exposure of 60 s. Since our study also involves acoustic streaming, we selected a pulse repetition frequency of 5 Hz with a 5% duty cycle to achieve a 10 ms pulse duration —optimizing mechanosensitive channel activation while mitigating heat generation. We applied a total sonication time of 20 s, which is shorter than but on the same order of magnitude as the 60 s used in their study. This duration proved sufficient to activate neurons without requiring prolonged ultrasound exposure.

Particle image velocimetry

Polystyrene beads (2 μm) suspension in 1 × DPBS (2.6% w/v) were used as tracers to map the flow field produced by the 25MHz ultrasound transducer in our experimental setup. The movement of tracer beads in the medium were recorded using a high-speed camera (Nova S12, Photron) at 12,800 frames per second with a 78 μs exposure time and were analyzed offline using the Particle Image Velocimetry (PIV) lab in MATLAB. Preprocessing was performed to locally enhance contrast using Contrast Limited Adaptive Histogram Equalization (CLAHE) with 64 pixels window size. Fast Fourier Transform (FFT) window deformation method was employed for the PIV setting with 3 passes and interrogation areas 80 × 80, 40 × 40 and 20 × 20 pixels with 50% overlap. The correlation robustness was set as "standard."

COMSOL multiphysics simulation

The numerical simulation was performed in COMSOL Multiphysics 6.0 trial version. The geometry was drawn according to the experimental setup and the focal length of the ultrasound transducer, where the sound waves incidents at a 45-degree angle, relative to the glass bottom of the recording chamber, and was reflected by the bottom. The computational fluid dynamic (CFD) module, acoustic module and the acoustic-fluid coupling module were selected for modeling. The 1st order acoustic fields (sound pressure and acoustic radiation force) were solved using the Thermos-viscous Acoustics interface in the Acoustics Module. The streaming flow was solved using the Laminar Flow physics interface of the CFD Module and the Acoustic-Fluid Coupling Module by adding the appropriate time-averaged, first-order sources: a mass source and a volume force. The results were obtained with transient analysis, and the time step was set to 1 ms. The initial velocity boundary condition was determined by adding appropriate velocity to the boundary of the ultrasonic transducer to match the PIV measurement.

Electrophysiological recording

Whole-cell patch-clamp recordings were acquired from single neurons via patch pipettes made from borosilicate glass (1.5 mm outer diameter, 0.84 mm inner diameter) pulled to resistances of 3–5 MΩ on a micropipette puller (PC-10, Narishige). Pipettes were filled with an intracellular solution containing (in mM): 135 K-Gluconate, 4 $MgCl_2$, 0.2 EGTA, 3 Na_2ATP, 0.3 Na_2GTP, and 10 HEPES, and PH adjusted to 7.25 with KOH, 291 mOsm. The extracellular solution contained (in mM): 150 NaCl, 3 KCl, 2 $CaCl_2$, 2 $MgCl_2$, 20 Glucose and 10 HEPES, PH adjusted to 7.35 with NaOH, 315 mOsm. An amplifier (Axon CNS MultiClamp 700B, Molecular Devices) was used to voltage clamp neurons at a holding potential of -70 mV. Recordings were digitized (Axon CNS Digidata 1440A, Molecular Devices), and data were acquired with pClamp software (Molecular Devices). All recordings were made at room temperature (21-25°C).

In some experiments, calcium-free external solution containing the calcium chelator EGTA (1mM) was used to test the role of calcium influx in ultrasound-evoked neurotransmitter release. To block EPSC evoked by action potentials, 1 μM tetrodotoxin (TTX) was added to the normal external solution. In other experiments, Kynurenic Acid (2 mM) was added to the normal external solution to suppress excitatory synaptic transmission. In all cases, care was taken to keep the external pH and osmolarity constant.

Calcium imaging

To load cells with the fluorescent calcium indicator dye, fluo-4, a cover slip of neuron culture was incubated with 1.25 μM fluo-4 AM (F14201, Thermo Fisher Scientific) in Neurobasal medium A (with 2% B27 and 1% 100X Glutamax) and incubated at 37°C in the dark for 15 min. Several (2–3 times) gentle washes with the normal external solution were used to remove unloaded fluo-4 AM before calcium imaging. The exposure out signal of the camera (Quantum 512SC) was connected to Digidata 1440A to precisely determine the timing of calcium images relative to electrophysiological signals.

Data analysis and statistics

Data was imported into Clampfit software (Molecular Devices) and MATLAB (R2018b, MathWorks) for analysis. The frequency of synaptic events was semi-automatically analyzed using the MATLAB based SpikeTrain function from Neurasmus B.V. One-way ANOVA multiple comparisons were used for statistical comparisons of the total charge of EPSC only or EPSC & AP between no US and US with lower, medium and higher intensity.

Conflict of interest

The authors declare that there is no conflict of interest regarding the publication of this article.

Acknowledgments

The authors thank Prof. Yufeng Zhou from Nanyang Technological University and Chongqing Medical University for providing equipment and guidance for the X-Y-Z acoustic output measurement of the US transducer, and Prof. Long Meng for the generous help of qualitative 3D mapping of US beam profile. The authors thank Melissa Yeow Wei Bao, Mengqin Wu, Minchuan Zhang, Chon U Chan and Vicky Liao for technical support, and Kai Voges for the generous gift of MATLAB based SpikeTrain function for EPSC analysis. This work was supported by the National Natural Science Foundation of China, Science Foundation for Youths (No. 12204322), the Natural Science Foundation of Guangdong province (No. 2023A1515010649), the Guangdong Provincial Pearl River Talents Program 2023QN10X235 and the LKCMedicine Dean's Postdoctoral Fellowship Grant from Nanyang Technological University Singapore, Singapore.

Data availability statement

Data will be made available on request.

Supplementary materials

Supplementary material associated with this article can be found in the online version at doi:10.1016/j.ultrasmedbio.2025.04.011.

References

[1] Wagner T, Valero-Cabre A, Pascual-Leone A. Noninvasive Human Brain Stimulation. Annual Review of Biomedical Engineering 2007;9(1):527–65.
[2] Blackmore J, Shrivastava S, Sallet J, Butler CR, Cleveland RO. Ultrasound Neuromodulation: A Review of Results, Mechanisms and Safety. Ultrasound Med Biol 2019;45(7):1509–36.
[3] Sharabi S, Daniels D, Last D, Guez D, Zivli Z, Castel D, et al. Non-thermal focused ultrasound induced reversible reduction of essential tremor in a rat model. Brain Stimulation 2019;12(1):1–8.
[4] Ye PP, Brown JR, Pauly KB. Frequency Dependence of Ultrasound Neurostimulation in the Mouse Brain. Ultrasound in Medicine & Biology 2016;42(7):1512–30.
[5] Kubanek J, Shukla P, Das A, Baccus SA, Goodman MB. Ultrasound elicits behavioral responses through mechanical effects on neurons and ion channels in a simple nervous system. The Journal of Neuroscience 2018;38(12):3081–91.
[6] Kim H, Taghados SJ, Fischer K, Maeng L-S, Park S, Yoo S-S. Noninvasive Transcranial Stimulation of Rat Abducens Nerve by Focused Ultrasound. Ultrasound in Medicine & Biology 2012;38(9):1568–75.
[7] Tufail Y, Matyushov A, Baldwin N, Tauchmann ML, Georges J, Yoshihiro A, et al. Transcranial Pulsed Ultrasound Stimulates Intact Brain Circuits. Neuron 2010;66(5):681–94.
[8] Lee W, Lee SD, Park MY, Foley L, Purcell-Estabrook E, Kim H, et al. Image-Guided Focused Ultrasound-Mediated Regional Brain Stimulation in Sheep. Ultrasound in Medicine and Biology 2016;42(2):459–70.
[9] Dallapiazza RF, Timbie KF, Holmberg S, Gatesman J, Lopes MB, Price RJ, et al. Noninvasive neuromodulation and thalamic mapping with low-intensity focused ultrasound. Journal of Neurosurgery 2018;128(3):875–84.
[10] Daniels D, Sharabi S, Last D, Guez D, Salomon S, Zivli Z, et al. Focused Ultrasound-Induced Suppression of Auditory Evoked Potentials. Ultrasound in Medicine and Biology 2018;44(5):1022–30.
[11] Kubanek J, Brown J, Ye P, Pauly KB, Moore T, Newsome W. Remote, brain region-specific control of choice behavior with ultrasonic waves. Sci Adv 2020;6(21):eaaz4193.
[12] Folloni D, Verhagen L, Mars RB, Fouragnan E, Constans C, Aubry JF, et al. Manipulation of Subcortical and Deep Cortical Activity in the Primate Brain Using Transcranial Focused Ultrasound Stimulation. Neuron 2019;101(6) 1109-+.
[13] Verhagen L, Gallea C, Folloni D, Constans C, Jensen DEA, Ahnine H, et al. Offline impact of transcranial focused ultrasound on cortical activation in primates. Elife 2019;8:e40541.
[14] Wattiez N, Constans C, Deffieux T, Daye PM, Tanter M, Aubry JF, et al. Transcranial ultrasonic stimulation modulates single-neuron discharge in macaques performing an antisaccade task. Brain Stimulation 2017;10(6):1024–31.
[15] Beisteiner R, Matt E, Fan C, Baldysiak H, Schonfeld M, Novak TPhilippi, et al. Transcranial Pulse Stimulation with Ultrasound in Alzheimer's Disease-A New Navigated Focal Brain Therapy. Adv Sci (Weinh) 2020;7(3):1902583.
[16] Legon W, Bansal P, Tyshynsky R, Ai L, Mueller JK. Transcranial focused ultrasound neuromodulation of the human primary motor cortex. Scientific Reports 2018;8(1):p10007.
[17] Legon W, Sato TF, Opitz A, Mueller J, Barbour A, Williams A, et al. Transcranial focused ultrasound modulates the activity of primary somatosensory cortex in humans. Nature Neuroscience 2014;17(2):322–9.
[18] Yoo S, Mittelstein DR, Hurt RC, Lacroix J, Shapiro MG. Focused ultrasound excites cortical neurons via mechanosensitive calcium accumulation and ion channel amplification. Nat Commun 2022;13(1):493.
[19] Sorum B, Rietmeijer RA, Gopakumar K, Adesnik H, Brohawn SG. Ultrasound activates mechanosensitive TRAAK K(+) channels through the lipid membrane. Proc Natl Acad Sci U S A 2021;118(6).
[20] Li F, Yang C, Yuan F, Liao D, Li T, Guilak F, et al. Dynamics and mechanisms of intracellular calcium waves elicited by tandem bubble-induced jetting flow. Proc Natl Acad Sci U S A 2018;115(3):E353–62.
[21] Li F, Park TH, Sankin G, Gilchrist C, Liao D, Chan CU, et al. Mechanically induced integrin ligation mediates intracellular calcium signaling with single pulsating cavitation bubbles. Theranostics 2021;11(12):6090–104.
[22] Plaksin M, Kimmel E, Shoham S. Cell-Type-Selective Effects of Intramembrane Cavitation as a Unifying Theoretical Framework for Ultrasonic Neuromodulation. eNeuro 2016;3(3) p. ENEURO.0136-15.2016.
[23] Plaksin M, Shoham S, Kimmel E. Intramembrane Cavitation as a Predictive Bio-Piezoelectric Mechanism for Ultrasonic Brain Stimulation. Physical Review X 2014;4(1):011004.
[24] Krasovitski B, Frenkel V, Shoham S, Kimmel E. Intramembrane cavitation as a unifying mechanism for ultrasound-induced bioeffects. Proceedings of the National Academy of Sciences of the United States of America 2011;108(8):3258–63.
[25] Tyler WJ, Tufail Y, Finsterwald M, Tauchmann ML, Olson EJ, Majestic C. Remote excitation of neuronal circuits using low-intensity, low-frequency ultrasound. PLoS One 2008;3(10):e3511.
[26] Min B-K, Yang PS, Bohlke M, Park S, Vago DR, Maher TJ, et al. Focused ultrasound modulates the level of cortical neurotransmitters: Potential as a new functional brain mapping technique. International Journal of Imaging Systems and Technology 2011;21(2):232–40.
[27] Xu T, Lu X, Peng D, Wang G, Chen C, Liu W, et al. Ultrasonic stimulation of the brain to enhance the release of dopamine - A potential novel treatment for Parkinson's disease. Ultrason Sonochem 2020;63:104955.
[28] Sato T, Shapiro MG, Tsao DY. Ultrasonic Neuromodulation Causes Widespread Cortical Activation via an Indirect Auditory Mechanism. Neuron 2018;98(5) p. 1031-+.
[29] Guo H, Hamilton M, Offutt SJ, Gloeckner CD, Li T, Kim Y, et al. Ultrasound Produces Extensive Brain Activation via a Cochlear Pathway. Neuron 2018;98(5):1020–1030.e4.
[30] Kop BR, Shamli Oghli Y, Grippe TC, Nandi T, Lefkes J, Meijer SW, et al. Auditory confounds can drive online effects of transcranial ultrasonic stimulation in humans. Elife 2024;12:RP88762.
[31] Dolphin AC, Lee A. Presynaptic calcium channels: specialized control of synaptic neurotransmitter release. Nature Reviews Neuroscience 2020;21(4):213–29.
[32] Augustine GJ, Charlton MP, Smith SJ. Calcium action in synaptic transmitter release. Annu Rev Neurosci 1987;10:633–93.
[33] Gitler D, Takagishi Y, Feng J, Ren Y, Rodriguiz RM, Wetsel WC, et al. Different presynaptic roles of Synapsins at excitatory and inhibitory synapses. Journal of Neuroscience 2004;24(50):11368–80.
[34] Bar-Yehuda D, Korngreen A. Space-clamp problems when voltage clamping neurons expressing voltage-gated conductances. J Neurophysiol 2008;99(3):1127–36.
[35] Williams SR, Mitchell SJ. Direct measurement of somatic voltage clamp errors in central neurons. Nat Neurosci 2008;11(7):790–8.
[36] Kim HJ, Phan TT, Lee K, Kim JS, Lee SY, Lee JM, et al. Long-lasting forms of plasticity through patterned ultrasound-induced brainwave entrainment. Sci Adv 2024;10(8):eadk3198.
[37] Van Hook MJ. Temperature effects on synaptic transmission and neuronal function in the visual thalamus. PLoS One 2020;15(4):e0232451.
[38] Barrett EF, Barrett JN, Botz D, Chang DB, Mahaffey D. Temperature-sensitive aspects of evoked and spontaneous transmitter release at the frog neuromuscular junction. J Physiol 1978;279:253–73.
[39] Lisman JE. Bursts as a unit of neural information: making unreliable synapses reliable. Trends Neurosci 1997;20(1):38–43.
[40] Chiappalone M, Vato A, Berdondini L, Koudelka-Hep M, Martinoia S. Network dynamics and synchronous activity in cultured cortical neurons. Int J Neural Syst 2007;17(2):87–103.
[41] Suresh J, Radojicic M, Pesce LL, Bhansali A, Wang J, Tryba AK, et al. Network burst activity in hippocampal neuronal cultures: the role of synaptic and intrinsic currents. J Neurophysiol 2016;115(6):3073–89.
[42] Bekkers JM, Stevens CF. Excitatory and inhibitory autaptic currents in isolated hippocampal neurons maintained in cell culture. Proc Natl Acad Sci U S A 1991;88(17):7834–8.
[43] Zhang Y, Rózsa M, Liang Y, Bushey D, Wei Z, Zheng J, et al. Fast and sensitive GCaMP calcium indicators for imaging neural populations. Nature 2023;615(7954):884–91.
[44] Grienberger C, Konnerth A. Imaging calcium in neurons. Neuron 2012;73(5):862–85.
[45] Zhu JJ, Xian QX, Hou XD, Wong KF, Zhu TT, Chen ZH, et al. The mechanosensitive ion channel Piezo1 contributes to ultrasound neuromodulation. Proceedings of the National Academy of Sciences of the United States of America 2023;120(18):e2300291120.
[46] Duque M, Lee-Kubli CA, Tufail Y, Magaram U, Patel J, Chakraborty A, et al. Sonogenetic control of mammalian cells using exogenous transient receptor potential A1 channels. Nature Communications 2022;13(1):600.
[47] Yang YH, Pacia CP, Ye DZ, Zhu LF, Baek H, Yue YM, et al. Sonothermogenetics for noninvasive and cell-type specific deep brain neuromodulation. Brain Stimulation 2021;14(4):790–800.
[48] Huang YS, Fan CH, Hsu N, Chiu NH, Wu CY, Chang CY, et al. Sonogenetic Modulation of Cellular Activities Using an Engineered Auditory-Sensing Protein. Nano Letters 2020;20(2):1089–100.
[49] Qiu ZH, Guo JH, Kala S, Zhu JJ, Xian QX, Qiu WB, et al. The Mechanosensitive Ion Channel Piezo1 Significantly Mediates Ultrasonic Stimulation of Neurons. Iscience 2019;21 p. 448-+.

[50] Ye J, Tang SY, Meng L, Li X, Wen XX, Chen SH, et al. Ultrasonic control of neural activity through activation of the mechanosensitive channel MscL. Nano Letters 2018;18(7):4148–55.
[51] Prieto ML, Firouzi K, Khuri-Yakub BT, Madison DV, Maduke M. Spike frequency–dependent inhibition and excitation of neural activity by high-frequency ultrasound. Journal of General Physiology 2020;152(11):e202012672.
[52] Prieto ML, Firouzi K, Khuri-Yakub BT, Maduke M. Activation of Piezo1 but Not Na(V) 1.2 Channels by Ultrasound at 43 MHz. Ultrasound Med Biol 2018;44(6):1217–32.
[53] Liao D, Li F, Lu D, Zhong P. Activation of Piezo1 mechanosensitive ion channel in HEK293T cells by 30 MHz vertically deployed surface acoustic waves. Biochemical and Biophysical Research Communications 2019;518(3):541–7.
[54] Collins MN, Mesce KA. Focused Ultrasound Neuromodulation and the Confounds of Intracellular Electrophysiological Investigation. eneuro 2020;7(4) ENEURO.0213-20.2020.
[55] Šponer J. Theoretical estimation of the cavitation threshold for very short pulses of ultrasound. Ultrasonics 1991;29(5):376–80.
[56] Lescrauwaet E, Vonck K, Sprengers M, Raedt R, Klooster D, Carrette E, et al. Recent Advances in the Use of Focused Ultrasound as a Treatment for Epilepsy. Frontiers in Neuroscience 2022;16.
[57] Zou JJ, Meng L, Lin ZR, Qiao YZ, Tie CJ, Wang YB, et al. Ultrasound Neuromodulation Inhibits Seizures in Acute Epileptic Monkeys. Iscience 2020;23(5):101066.
[58] Bianchi D, Marasco A, Limongiello A, Marchetti C, Marie H, Tirozzi B, et al. On the mechanisms underlying the depolarization block in the spiking dynamics of CA1 pyramidal neurons. Journal of Computational Neuroscience 2012;33(2):207–25.
[59] Augustine GJ, Charlton MP, Smith SJ. Calcium entry and transmitter release at voltage-clamped nerve terminals of squid. J Physiol 1985;367:163–81.
[60] Heidelberger R, Heinemann C, Neher E, Matthews G. Calcium dependence of the rate of exocytosis in a synaptic terminal. Nature 1994;371(6497):513–5.
[61] Fan WY, Chen YM, Wang YF, Wang YQ, Hu JQ, Tang WX, et al. L-Type Calcium Channel Modulates Low-Intensity Pulsed Ultrasound-Induced Excitation in Cultured Hippocampal Neurons. Neurosci Bull 2024;40(7):921–36.
[62] Niu X, Yu K, He B. Transcranial focused ultrasound induces sustained synaptic plasticity in rat hippocampus. Brain Stimul 2022;15(2):352–9.
[63] Bi GQ, Poo MM. Synaptic modifications in cultured hippocampal neurons: dependence on spike timing, synaptic strength, and postsynaptic cell type. J Neurosci 1998;18(24):10464–72.
[64] Liao D, Hsiao MY, Xiang G, Zhong P. Optimal pulse length of insonification for Piezo1 activation and intracellular calcium response. Sci Rep 2021;11(1):709.